

Diffractive Microlensing I: Flickering Planetesimals at the Edge of the Solar System

Jeremy Heyl

*Department of Physics and Astronomy, University of British Columbia, Vancouver, British Columbia, Canada, V6T 1Z1;
Email: heyjl@phas.ubc.ca; Canada Research Chair*

Accepted 2009 November 26. Received 2009 November 23; in original form 2009 October 20

ABSTRACT

Microlensing and occultation are generally studied in the geometric optics limit. However, diffraction may be important when recently discovered Kuiper-Belt objects (KBOs) occult distant stars. In particular the effects of diffraction become more important as the wavelength of the observation and the distance to the KBO increase. For sufficiently distant and massive KBOs or Oort cloud objects not only is diffraction important but so is gravitational lensing. For an object similar to Eris but located in the Oort cloud, the signature of gravitational lensing would be detected easily during an occultation and would give constraints on the mass and radius of the object.

Key words: Kuiper Belt — Solar System : minor planets, asteroids — Solar System : Oort Cloud — Solar System : gravitational lensing

1 INTRODUCTION

Bailey (1976) first argued that small bodies in the distant solar system could be detected through stellar occultations. Roques et al. (1987) developed the treatment of occultation by irregular bodies including diffraction. More recently with the discovery of the population of Kuiper Belt objects (Kuiper 1951; Jewitt 1999), several research groups have begun searching for more distant and smaller bodies through occultations (Roques & Moncuquet 2000; Bickerton et al. 2008; Roques et al. 2009). Because Kuiper Belt objects (KBOs) typically subtend small angles, the diffraction of radiation around the objects may be important even at visible wavelengths and naturally more important at longer wavelengths (Roques et al. 1996). The discovery of more distant and more massive KBOs such as Eris (Brown et al. 2005) begs the question of whether gravitational lensing of background stars by large KBOs and objects in the Oort cloud (Oort 1950) is important. Cooray (2002) argued that for distant massive KBOs and Oort cloud objects lensing may be important; furthermore, Gaudi & Bloom (2005) argued that GAIA could measure the astrometric displacement from microlensing by an planet more massive than a few Jupiters within 10^4 AU regardless of its location on the sky. The technique in this paper

probes much lower mass objects, but also exploits lensing to provide constraints on the properties of the asteroid.

Generally the diffractive effects of microlensing are neglected because the variation in the time delays across the lens is usually much larger than the coherence time of the observation, $1/\Delta\nu$ where $\Delta\nu$ is the bandwidth of the observation. However, near a caustic crossing, diffraction may be important as argued by Jaroszynski & Paczynski (1995) to account for rapid variations in the light from Q2237+0305 (The Einstein Cross). Typically the differential time delay highly magnified images for a point lens is about $2GM/c^3$, the crossing time over the Schwarzschild radius of the lens; consequently, for the diffractive effects of lensing to be observable the Schwarzschild radius of the lens should be comparable or larger than the wavelength of the radiation. The largest of the Kuiper Belt objects, Eris, has a Schwarzschild radius $R_S = 2GM/c^2 \approx 25\mu\text{m}$. Therefore, quite naturally for observations of large KBOs diffractive microlensing may be important for observations in the near and mid-infrared whenever the gravitational effects are important. This paper focuses on just this regime.

The first section, §2, outlines microlensing in the diffractive regime and generalizes the earlier results to include occultation. This yields an expression for the transmission that is nearly identical to the unlensed result. The next section, §3,

outlines the types of objects for which diffractive lensing may be important, examines several interesting cases and connects the diffraction patterns to the geometric limit (§2.2) in the limit where the lensing is weak. The final section (§4) outlines how diffractive lensing could constrain the properties of known objects and speculates on the probability of such lensing events.

2 DIFFRACTIVE MICROLENSING

The following definitions will prove useful throughout the paper. The source lies a distance v in the plane of the sky from the centre of the lensing occulter. The variable u is a radial variable over the plane containing the lensing occulter and φ gives the polar angle in this plane with $\varphi = 0$ pointing toward the projection of the source onto this plane. The magnification is given by squared modulus of the integral over the phases in the lens plane (Schneider et al. 1992)

$$\mu_\omega = \left| \int_{u_d}^{\infty} du u^{1-if} e^{iu^2/2} \int_0^{2\pi} d\varphi e^{-ifuv \cos \varphi} \right|^2. \quad (1)$$

The lower bound accounts for the effects of occultation with

$$u_d = r_d \sqrt{\frac{\omega_d}{c} \frac{D_s}{D_d D_{ds}}}. \quad (2)$$

where r_d is the radius of the occulter and ω_d is the angular frequency of the radiation at the lensing occulter. The value u_d is related to the Fresnel number such that $F = u_d^2/(2\pi)$. The other parameter is $f = 2R_S \omega_d/c$ ($R_S = 2GM_d/c^2$) where M_d is the mass of the occulter. The Einstein radius is the characteristic length of the lens,

$$R_E = \sqrt{2R_S \frac{D_d D_{ds}}{D_s}} = \frac{\sqrt{f}}{u_d} r_d. \quad (3)$$

Performing the angular integral yields

$$\mu_\omega = \left| \int_{u_d}^{\infty} u^{1-if} e^{iu^2/2} J_0(uv) du \right|^2. \quad (4)$$

The limit where the gravitational field of the lens is negligible is $f = 0$, so the effect of gravity on the form of the integral is quite modest.

2.1 Evaluating the Integral

The integral can be calculated in closed form in terms of the confluent hypergeometric function (${}_1F_1(a; b; z)$) for $u_d = 0$. Using relation (6.631.1) from Gradshteyn & Ryzhik (1994) yields

$$\int_0^{\infty} u^{1-if} e^{iu^2/2} J_0(uv) du = e^{\pi f/4} e^{i(\pi - f \ln 2)/2} \Gamma\left(1 - i\frac{f}{2}\right) \times {}_1F_1\left(1 - i\frac{f}{2}; 1; -i\frac{v^2}{2}\right). \quad (5)$$

The result for $f = 0$ is simply $i \exp(-iv^2/2)$. These analytic results are used to calculate the integral in Eq. (4), both with

and without lensing. Rather than performing the integration to $u \rightarrow \infty$, the result of the integration from $u = 0$ to $u = u_d$ is subtracted from Eq. 5.

2.2 Geometric Optics

To compare with the standard, high frequency results for lensing and occultation (e.g. Agol 2002), the geometric limit is useful. In the geometric limit the images are located at those places in the image plane u where the phase in the integral for μ_ω is stationary, so $v = u - f/u$, yielding two image positions,

$$u_\pm = \frac{1}{2} \left(v \pm \sqrt{v^2 + 4f} \right), \quad \phi = 0 \quad (6)$$

with the magnifications

$$\mu_\pm = \frac{u_\pm}{v} \left| \frac{du_\pm}{dv} \right| = \frac{1}{2} \left(\frac{v^2 + 2f}{v\sqrt{v^2 + 4f}} \pm 1 \right). \quad (7)$$

The size of the Einstein radius in these units is simply \sqrt{f} , so if $\sqrt{f} \gtrsim u_d$ one expects that lensing will be important. To account for the occultation in the limit of a point source, the only the magnification for images with $u_\pm > u_d$ is included (Agol 2002). As the following section will show, the geometric optics approximation not only provides an estimate of the magnification but it also provides a mapping to convert an unlensed diffraction pattern to an approximation of the lensed pattern through the locations of images in Eq. (6).

3 RESULTS

Because Kuiper Belt objects provide the inspiration for this work, it is natural to take the largest KBO, Eris, as an exemplar. Eris is a dwarf planet orbiting the Sun at a distance of up to 100 AU. Its radius is about 1200 km (Brown et al. 2006; Stansberry et al. 2008), yielding a value of $u_d = 770$ at one micron and a Fresnel number of about 10^5 . Its mass is about 1.7×10^{25} g (Brown & Schaller 2007) so its Schwarzschild radius is about 25 microns so $f \approx 310$ at one micron. At one hundred AU, the diffractive effects are not important over a reasonable bandwidth. Furthermore, $u_d \gg \sqrt{f}$ so microlensing is not important either.

On the other hand, Eris is likely to be one of the closest and biggest members of a large population of KBOs and Oort cloud objects. Eris provides a fiducial density of about 2.3 g cm^{-3} (about one-half that of Earth, 5.5 g cm^{-3}) to examine a variety of objects at various distances and sizes and determine the possible regimes where microlensing and diffraction could both be important. Fig. 1 examines the various regimes using the fiducial density of Eris and a wavelength of one micron. The values of f and u_d^2 at one micron are depicted on the figure, and they both scale inversely with wavelength. In particular to exploit the point-source approximation in the previous section, the angular size of the object or the angular size of the object's Einstein radius should be greater than the angular size of the typical source (for example, a solar-type

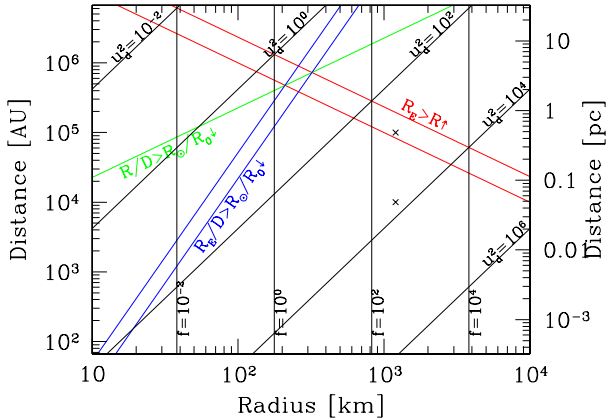


Figure 1. The values of f and u_d^2 as a function of the radius of the asteroid and its distance for $\lambda = 1\mu\text{m}$. Both f and u_d^2 scale as λ^{-1} . The green line $R/D > R_\odot/R_0$ indicates the region where the angular size of the asteroid exceeds that of a solar-type star in the bulge, so the point-source approximation for occultation is valid. The blue line $R_E/D > R_\odot/R_0$ indicates the region where the angular size of the Einstein radius of the asteroid exceeds that of a solar-type star in the bulge, so the point-source approximation for microlensing is valid. The red line $R_E > R$ indicates the region where the Einstein radius is larger than the radius of the object so lensing will dominate over occultation. In the latter two cases the density of the asteroid is assumed to be equal that of Eris. A second line to the left gives the boundary for an asteroid 2.3 times denser similar to the density of Earth. The upper cross indicates the parameters for Figs. 2 and 3. The lower cross gives the parameters for Fig. 4.

star in the bulge taken to be 7.6 kpc away). In the figure the point-source approximation is valid for objects that lie either to the right of the green line or the blue lines (the left-hand blue line uses Earth’s mass density). Microlensing becomes important for objects near or above the red lines (the lower red line uses Earth’s mass density).

The figure indicates that observations of Eris at the distance of 100 AU give $u_d^2 \approx 10^6$ at one micron and $f \approx 10^{2.5}$, so $u_d^2 \gg f \gg 1$ so neither lensing nor diffraction are important for Eris, as discussed earlier (at least at one micron — Eris will diffract for $\lambda \gtrsim 1\text{m}$). On the other hand, if there were an Eris-like object at 10^5 AU (upper cross) and it were observed at ten microns, $u_d = 7.8$ and $f \approx 31.4$, yielding interesting diffractive effects over a reasonable bandwidth. At this distance Eris would subtend about 1.7×10^{-10} radians, larger than any sun-like star beyond a few hundred parsecs, so the star can be taken to be a point source. At 10^5 AU the asteroid is essentially beyond the realm of the solar system as passing molecular clouds would unbind objects beyond 4×10^4 AU (Bailey 1983). Because this is a statistical process, some objects would remain but they would be quite rare.

Regardless of the paucity of objects at this distance, an Eris-like object at 10^5 AU provides an excellent illustration of diffractive microlensing and occultation. Beyond a distance of one parsec, Eris would no longer fully occult a star because

even when fully aligned the lensing would be sufficient to bend the light around the limb of Eris and toward Earth. Even at this distance solar-like stars beyond a kiloparsec would be essentially point sources for the purposes of the lensing signature. Furthermore, the diffraction pattern depends on the values of u_d and f , so it would also apply to more massive and nearer objects but at larger wavelengths — for example, observations of an object like Earth at 85 GHz from a distance of 8,000 AU give the same set of values.

Although such objects would be difficult to detect and the possibility of an occultation event for a given object would be small, the properties of an occultation and microlensing event for an Eris-like object at 10^4 and 10^5 AU are extremely illustrative. At 10^5 AU, diffraction is important even at one micron. Fig. 2 gives the diffraction and lensing pattern for an Eris-like asteroid at 10^5 AU at one and ten microns. The complete diffraction pattern including the effects of gravitational lensing is given in black. The diffraction pattern with $f = 0$ (no lensing) is given in red. The diffraction pattern including lensing oscillates about the geometric-optics value of the microlensing magnification (green curve) from Eq. (7). One can obtain an approximate idea of the diffraction pattern including lensing by using the lensing mapping *i.e.* $v \rightarrow v - f/v$ and taking the product of the geometric magnification with the unlensed diffraction pattern resulting in the blue curve. When the lensing effect is weak as in Fig. 4, this *a posteriori* lensing correction works quite well, so occultation diffraction patterns can be corrected for a modest amount of lensing without calculating the full lensing diffraction pattern. However, this mapping fails to reproduce the central fringing that occurs when both diffraction and lensing are important.

Averaging the magnification over a finite bandwidth smooths out much of the small-scale oscillation in the light curves as shown in Fig. 3. However, even over a moderate bandwidth of twenty-percent the microlensed diffraction patterns are easily distinguished from the unlensed patterns. Again the lensing mapping does a reasonable job of reproducing the pattern. This important to emphasise. Microlensing does not simply contract the diffraction pattern so it is not covariant with varying the relative velocities of the lens, source and detector nor is it covariant with varying the impact parameter of the occultation (how close to exactly aligned the source, lens and detector become). The lensing both increases the amplitude of the diffractive oscillations and shifts the locations of the peaks and troughs in a non-trivial manner, following the lensing mapping if the lensing is weak.

If the Eris-like asteroid were closer to Earth at 10^4 AU, Fig 1 indicates that the lensing would be weaker (the lower cross is well below the red lines). The results depicted in Fig. 4 bear this out. The location of the first peak moves inward from $1.09u_d$ to $1.04u_d$ because the light is slightly bent about the limb of the asteroid, decreasing the duration of the occultation by about 4.8%, approximately the value of $f/u_d^2 \approx 5.2\%$.

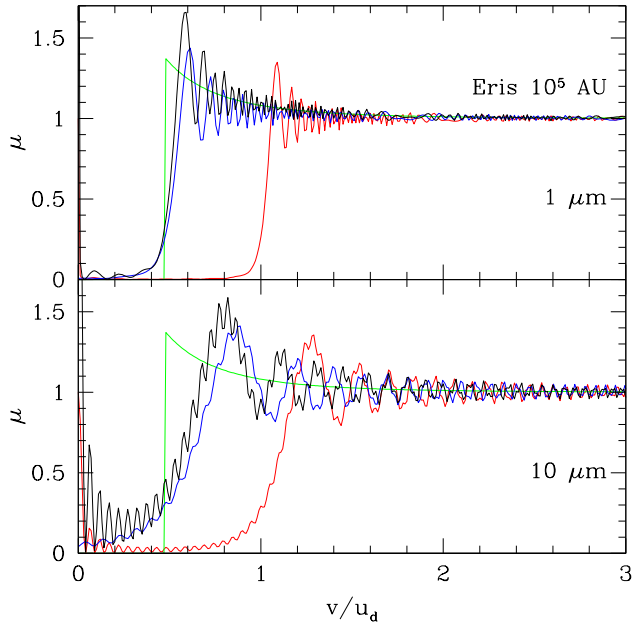


Figure 2. The magnification μ as a function of the location of the source (v) for an Eris-like object at 10^5 AU about 0.5 pc. The value of $v = u_d$ just as the source passes behind the edge of the occulter. For $v = 0$ the source lies directly behind the centre of the circular occulter. The black curve gives the magnification including gravitational lensing. The red curve gives the standard Fresnel diffraction result. The green curve gives the microlensing magnification in the geometric optics limit, and the blue curve gives the lensed version of the unlensed diffraction pattern (see text). The observations lie at one and ten microns and have zero bandwidth. The upper panel gives $\lambda = 1\mu\text{m}$ ($f = 314$ and $u_d = 25.$) and the lower panel gives $\lambda = 10\mu\text{m}$ ($f = 31.4$ and $u_d = 7.8$).

4 CONCLUSIONS

Microlensing is important for large asteroids (similar to Eris) in the Oort cloud and beyond; furthermore, in the near infrared and red-ward diffraction is important to understand the light curves from the combined microlensing and occultation of background stars by such objects. The effects of microlensing are not covariant with variations in the velocity of source, lens and observer nor with variations in the impact parameter; therefore, observations of diffractive lensing combined with a measured distance to the asteroid constrain the mass and radius of the asteroid, or equivalently with an assumed value of the density of the asteroid, such observations would yield a mass, radius and distance. Observations of diffractive microlensing may provide the only way of estimating the masses of such objects unless they have a satellite as Eris does (Brown & Schaller 2007).

The angular size of even a large asteroid such as Eris is extremely small at the distance of the Oort cloud, so one would expect that the chance for an occultation would be tiny. Over

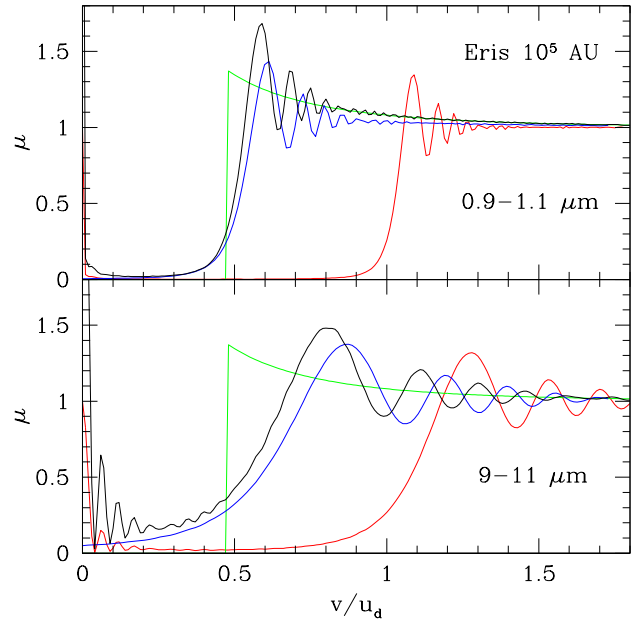


Figure 3. Same as Fig 2 but for a twenty-percent bandwidth.

the course of a year, the asteroid will sweep out a region of the sky. The chance of detection each year is proportional to this area. The semimajor axis of the annual parallactic ellipse on the sky ranges from two to twenty arcseconds for a distance of 10^5 and 10^4 AU respectively. The area of sky covered each year is given by the product of the arclength around the parallactic ellipse and angular diameter of the asteroid about 0.33 mas for an asteroid of radius 1200 km at 10^4 AU; therefore, on average, at the nearer distance the asteroid would cover a region of sky 0.33 mas by 100 arcseconds or about 0.033 square arcseconds or a fraction 6×10^{-14} of the entire sky each year. The solid angle covered decreases inversely with the distance squared until microlensing starts to dominate, subsequently the area is proportional to $d^{-3/2}$. It is safe to assume that the asteroid has sufficient velocity perpendicular to the Earth's orbital motion that it moves much more than one diameter per year (much greater than 8.2 cm/s); therefore, the asteroid will cover a new region each year. The asteroid itself may have a large proper motion that could increase the area further — this motion is neglected in this analysis. Any star within this area of sky will pass within the region $v < u_d$ in Figs. 2 through 4 over the course of that year. If one assumes that the Oort cloud contains about ten Earth masses of objects similar to Eris at about 10^4 AU, one would have to monitor about 4×10^8 stars for twelve years (twenty-four hours per day) to find a single microlensing occultation event by an object at 10^4 AU. The motion of the Earth in its orbit determines the duration of the event of about a minutes.

Currently the OGLE collaboration monitors about 4×10^8 stars — the present state of the art. OGLE-III ran from 2001

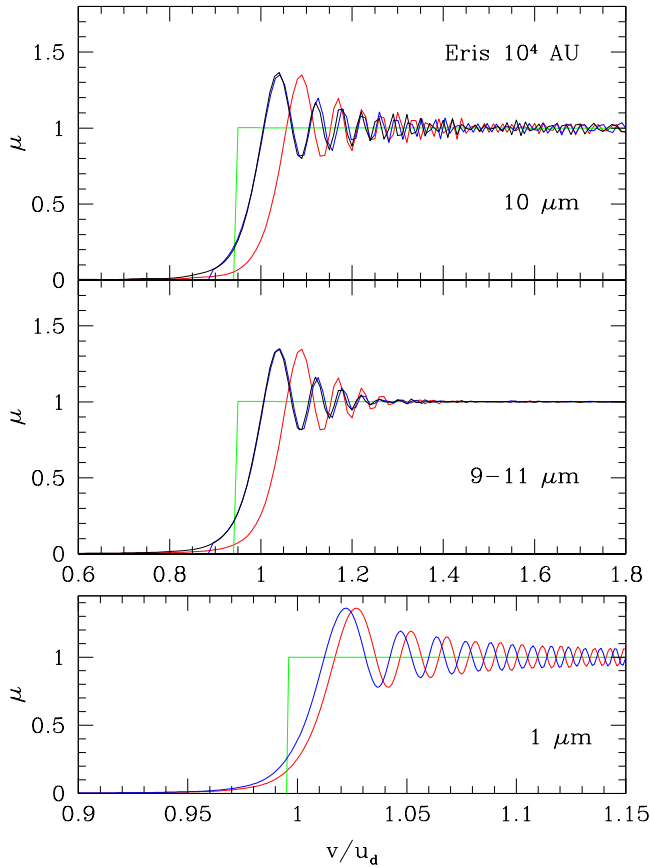


Figure 4. The upper panel gives the zero bandwidth results for ten microns and $d = 10^4$ AU (similar to the lower panel of Fig. 2 but for $f = 31.4$ and $u_d = 25$), and the middle panel gives the same results averaged over a twenty-percent bandwidth (similar to the lower panel of Fig 3). The x -axis starts at $v/u_d = 0.6$ unlike in the previous figures. The blue and black curves nearly coincide. The lower panel gives the results for $1 \mu\text{m}$. At one micron the direct calculation including lensing becomes nearly intractable; however, the lensing effect is weak so the *a posteriori* lensing correction provides a good approximation.

to 2009 and made nearly 2×10^{11} photometric measurements (Udalski et al. 2008). The key is not only the sensitivity of the current slew of experiments, although monitoring additional stars or using several telescopes separated by at least the diameter of the asteroid would increase the detection rate, but the cadence of OGLE-III at about five minutes would simply undersample and miss such an event. OGLE-IV will provide both a higher sensitivity and a higher cadence, but probably not a rapid enough cadence to distinguish such an event. The best approach would be a difficult hybrid of the high cadence of observations such as Roques et al. (2006) on a large telescope and the monitoring of many stars as OGLE. Because the goal is not small bodies as in Roques et al. (2006), a 21ms-cadence is overkill; a one-second cadence would be sufficient allowing

observations of much fainter stars. Furthermore, stars with especially small angular sizes are not necessary. Both of these factors along with the dedicated use of a large telescope could make probing the largest and presumably the rarest objects in the Oort cloud possible.

ACKNOWLEDGMENTS

The Natural Sciences and Engineering Research Council of Canada, Canadian Foundation for Innovation and the British Columbia Knowledge Development Fund supported this work. This research has made use of NASA's Astrophysics Data System Bibliographic Services. I would also like to thank the referee for many useful suggestions.

REFERENCES

- Agol E., 2002, *The Astrophysical Journal*, 579, 430
 Bailey M. E., 1976, *Nature*, 259, 290
 Bailey M. E., 1983, *Monthly Notices*, 204, 603
 Bickerton S. J., Kavelaars J. J., Welch D. L., 2008, *Astron. J*, 135, 1039
 Brown M. E., Schaller E. L., 2007, *Science*, 316, 1585
 Brown M. E., Schaller E. L., Roe H. G., Rabinowitz D. L., Trujillo C. A., 2006, *Astrophys. J Lett*, 643, L61
 Brown M. E., Trujillo C. A., Rabinowitz D. L., 2005, *Astrophys. J Lett*, 635, L97
 Cooray A., 2002, *ArXiv Astrophysics e-prints*, astro-ph/0209545
 Gaudi B. S., Bloom J. S., 2005, *Astrophys. J*, 635, 711
 Gradshteyn I. S., Ryzhik I. M., 1994, *Table of Integrals, Series, and Products*, fifth edn. Academic Press
 Jaroszynski M., Paczynski B., 1995, *Astrophys. J*, 455, 443
 Jewitt D., 1999, *Annual Review Of Earth And Planetary Sciences*, 27, 287
 Kuiper G. P., 1951, *Proceedings of the National Academy of Sciences of the United States of America*, 37, 1
 Oort J. H., 1950, *Bull. Astron. Inst. Neth.*, 11, 91
 Roques F., Boissel Y., Doressoundiram A., Sicardy B., Widemann T., 2009, *Earth*, 105, 201
 Roques F., et al., 2006, *Astron. J*, 132, 819
 Roques F., Moncuquet M., 2000, *Icarus*, 147, 530
 Roques F., Moncuquet M., Sicardy B., 1987, *Astron. J*, 93, 1549
 Roques F., Moncuquet M., Sicardy B., 1996, *Astronomical Journal*, 93, 1549
 Schneider P., Ehlers J., Falco E. E., 1992, *Gravitational Lenses*. Springer, Berlin
 Stansberry J., Grundy W., Brown M., Cruikshank D., Spencer J., Trilling D., Margot J., 2008, *Physical Properties of Kuiper Belt and Centaur Objects: Constraints from the Spitzer Space Telescope*. pp 161–179
 Udalski A., Szymanski M. K., Soszynski I., Poleski R., 2008, *Acta Astronomica*, 58, 69